DOI: 10.1002/chem.200902873

A Computational Study of the Olefin Epoxidation Mechanism Catalyzed by Cyclopentadienyloxidomolybdenum(VI) Complexes

Aleix Comas-Vives,[a] Agustí Lledós,*[a] and Rinaldo Poli*[b, c]

Abstract: A DFT analysis of the epoxidation of C_2H_4 by H_2O_2 and MeOOH (as models of *tert*-butylhydroperoxide, TBHP) catalyzed by [Cp*MoO_2Cl] (**1**) in $CHCl_3$ and by [Cp*$MoO_2(H_2O)$]$^+$ in water is presented (Cp* = pentamethylcyclopentadienyl). The calculations were performed both in the gas phase and in solution with the use of the conductor-like polarizable continuum model (CPCM). A low-energy pathway has been identified, which starts with the activation of ROOH (R = H or Me) to form a hydro/alkylperoxido derivative, [Cp*MoO(OH)(OOR)Cl] or [Cp*MoO(OH)(OOR)]$^+$ with barriers of 24.9 (26.5) and 28.7 (29.2) kcal mol^{-1} for H_2O_2 (MeOOH), respectively, in solution. The latter barrier, however, is reduced to only 1.0 (1.6) kcal mol^{-1} when one additional water molecule is explicitly included in the calculations. The hydro/alkylperoxido ligand in these intermediates is η^2-coordinated, with a significant interaction between the Mo center and the O^β atom. The subsequent step is a nucleophilic attack of the ethylene molecule on the activated O^α atom, requiring 13.9 (17.8) and 16.1 (17.7) kcal mol^{-1} in solution, respectively. The corresponding transformation, catalyzed by the peroxido complex [Cp*$MoO(O_2)Cl$] in $CHCl_3$, requires higher barriers for both steps (ROOH activation: 34.3 (35.2) kcal mol^{-1}; O atom transfer: 28.5 (30.3) kcal mol^{-1}), which is attributed to both greater steric crowding and to the greater electron density on the metal atom.

Keywords: density functional calculations · epoxidation · homogeneous catalysis · molybdenum · oxido ligands

Introduction

The olefin epoxidation reaction is extremely important as a relatively easy way to access functionalized organic materials from crude oil fractions. The reaction occurs with organic peroxides such as peracids and dioxiranes without the need for a catalyst.[1] The metal-catalyzed version has attracted much attention due to the possibility of performing more selective, notably enantioselective, transformations. Among the possible oxygen-delivering agents, H_2O_2 is the subject of the greatest number of investigations,[2] due to its low cost and easy availability. However, *tert*-butylhydroperoxide (TBHP) is still heavily used in the research laboratory and industrially, because it generally outperforms hydrogen peroxide. Many transition-metal catalysts have been used to carry out this transformation, including high oxidation state oxido complexes (methyltrioxidorhenium, dioxido derivatives of Mo and W),[3–7] bis(peroxido) complexes [$(L^1)(L^2)MO(O_2)_2$] (M = Mo, W),[8] polyoxometallates,[9–11] a variety of oxido complexes generated in situ from Fe and Mn porphyrin, salen, and other coordination compounds.[12–15]

The mechanism of this reaction has been, and continues to be, a controversial subject. In many cases, a mechanism related to that accepted for organic peracids is proposed[16] (Scheme 1a). However, this mechanism is easily understood only when H_2O_2 is the oxidant, because the active M–OOH species, (Scheme 1b), can be regenerated from the hydroxido product, M–OH, by simple ligand exchange.[17] It cannot

[a] Dr. A. Comas-Vives, Prof. A. Lledós
Unitat de Química Física, Departament de Química
Edifici Cn, Universitat Autònoma de Barcelona
08193 Bellaterra, Catalonia (Spain)
Fax: (+34) 93581292
E-mail: agusti@klingon.uab.es

[b] Prof. R. Poli
CNRS, LCC (Laboratoire de Chimie de Coordination)
Université de Toulouse, UPS, INP, 205, route de Narbonne
31077 Toulouse, 08193 (France)
Fax: (+33) 561553003
E-mail: rinaldo.poli@lcc-toulouse.fr

[c] Prof. R. Poli
Institut Universitaire de France
103, bd Saint-Michel, 75005 Paris (France)

Supporting information for this article is available on the WWW under http://dx.doi.org/10.1002/chem.200902873.

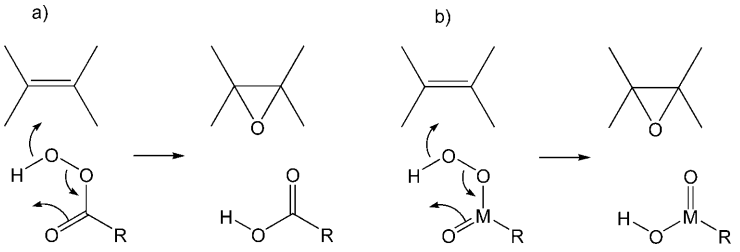

Scheme 1.

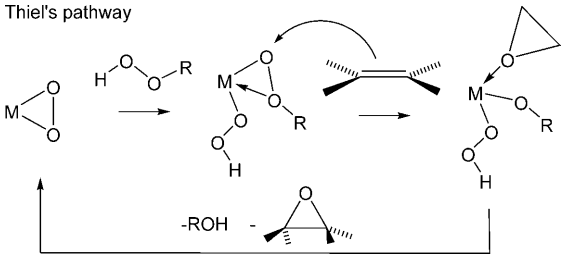

Scheme 3.

be the operative mechanism for the reactions using TBHP unless a second oxygen atom transfer takes place to regenerate the active M–OOH species from TBHP and M–OH.

The fact that a large number of peroxido complexes of molybdenum and tungsten have been isolated and fully characterized[18] has led to the idea that a peroxido ligand is capable of transferring an oxygen atom to the olefin. Two reference mechanisms are based on this idea, usually referred to as the "Mimoun"[19] and "Sharpless"[20] mechanisms (Scheme 2). Once again, for the reasons outlined

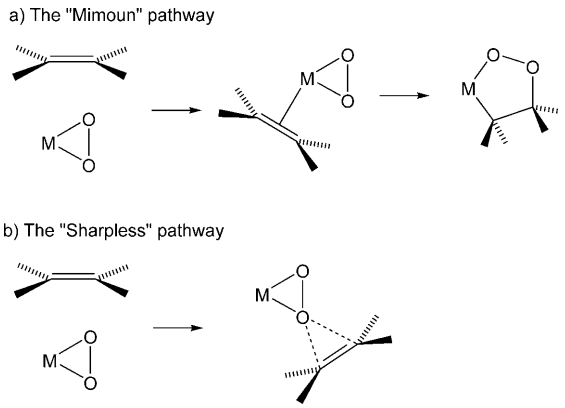

Scheme 2.

above, these two mechanisms are easily understood only when H_2O_2 is used, and are less so when TBHP is involved.

A number of theoretical investigations have addressed the two competing mechanisms shown in Scheme 2, mostly for Mo,[21–29] but also for other metals,[30,31] leading to a clear preference for the Sharpless scheme. The need to modify these mechanisms in order to account for the activity of TBHP has been presented by Thiel,[32–34] but to the best of our knowledge no thorough theoretical investigation has followed. Thiel's proposal is outlined in Scheme 3. Essentially, the peroxido ligand serves as a depository of the reactant's proton. The oxidizing agent is activated by coordination, and becomes susceptible to nucleophilic attack by the olefin at the electrophilic oxygen atom. Note that this mechanism, proposed by Thiel for the specific oxidation with TBHP (R = *t*Bu), may also operate for H_2O_2 (R = H). Note also that the basic principle is identical to that proposed by Sharpless (exogenous attack of the olefin at an electrophilic oxygen atom, without coordination). However, the oxygen is not transferred from a coordinated peroxido ligand, rather from the *tert*-butylperoxido (or hydroperoxido) ligand. Finally, note that other metal-bonded functionalities may exert, in principle, the same proton depository function (for instance, oxido ligands).

Extensive experimental studies carried out with $[MoO_2X_2L_2]$-type catalysts and TBHP as oxidant have shown that the source of the oxygen atom for the epoxidation is TBHP and not the catalyst's oxido ligands, ruling out the possible involvement of direct oxygen atom transfer from $Mo(O_2)$ moieties, and invalidating both Mimoun and Sharpless mechanisms as originally proposed.[35] Thus, the existence and stability of peroxido complexes must be related to side processes, such as the deprotonation of hydroperoxido ligands, Mo–OOH. Indeed, a study by Bergman (the first catalytic study using an organometallic oxido derivative of molybdenum) showed that the [Cp*MoO_2Cl]/TBHP (Cp* = pentamethylcyclopentadienyl) system is effective for olefin epoxidation, whereas the peroxido analogue, [Cp*$MoO(O_2)Cl$], is catalytically inactive.[36] Thus, the peroxido compound cannot be implicated as a catalytic intermediate in the [Cp*MoO_2Cl]-catalyzed epoxidation with TBHP. These findings were later confirmed by Roesky, who also reported the X-ray structure of the [Cp*$MoO(O_2)Cl$] compound.[37] Subsequent studies by Kühn and Romão have shown that related complexes with different cyclopentadienyl ligands, as well as alkyl derivatives of type [$Cp^{\#}MoO_2R$] ($Cp^{\#}$ = substituted cyclopentadienyl ligand, R = alkyl) are also catalytically active.[38–40] In a recent collaborative study, some of us showed that the dinuclear oxido-bridged [$Cp^{\#}_2Mo_2O_5$] systems are also catalytically active when using TBHP in an organic solvent, and are active with the same reagent under aqueous biphasic conditions.[41] However, they do not yield significant amounts of epoxidation product when TBHP is replaced by H_2O_2.[42]

Only recently, the use of MeOOH as a model of the *t*BuOOH reagent has been considered in a theoretical study, based on the compound [MoO_2Br_2(MeN=CHCH=NMe)] as the catalyst.[35,43] The activation step of the oxidant reported by this study resembles that proposed by Thiel, except that an oxido ligand is used as the proton depository (see Scheme 4). Hydrogen bonding between the hydroxido proton and the O^{β} atom of the organoperoxido ligand was found to stabilize this intermediate. However, the subse-

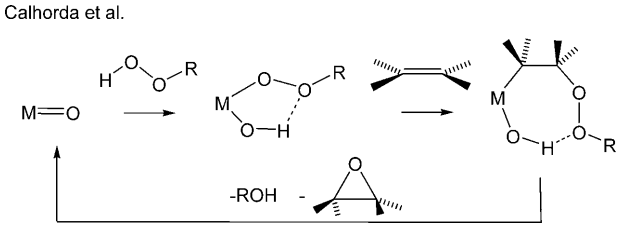

Scheme 4.

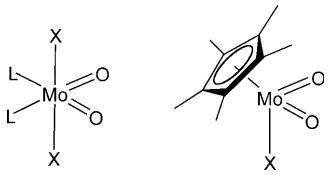

Scheme 5.

quent step of the mechanism is quite different than that proposed by Thiel, and involves an insertion into the metal–peroxido bond, similar to the pathway proposed by Mimoun (though preliminary olefin coordination does not occur). The most puzzling feature of this mechanism is that the olefin insertion transition state is calculated as 52 kcal mol^{-1} higher in energy (63 kcal mol^{-1} higher in free energy) than the intermediate, which is itself 16 kcal mol^{-1} higher in energy (29 kcal mol^{-1} higher in free energy) than the starting materials (catalyst + MeOOH + olefin). This is a prohibitive activation barrier for an efficient catalytic process. For this reason, we thought that a new theoretical investigation of the epoxidation mechanism was warranted.[44]

We are interested in the aqueous chemistry of the Cp*Mo^{VI} system[45] and have shown that compound [Cp*$_2$Mo$_2$O$_5$] self-ionizes in water to yield a 1:1 mixture of [Cp*MoO$_2$(H$_2$O)]$^+$ and [Cp*MoO$_3$]$^-$, which then evolves to a different ratio by spontaneous hydrolysis or by adjustment of the pH with a buffer.[46] Although the dinuclear compound may exert the same mechanistic function as [Cp*MoO$_2$Cl] (the Cl ligand being replaced by the oxido-bridged Cp*MoO$_3$ group), only the cationic complex is likely to exert a catalytic function among the charged species, because the water ligand can dissociate rather easily[47] and the resulting coordination site may be used for the oxidant activation. Useful background information comes from our recent computational study of hydration and proton transfer processes for the [Cp*MoO$_2$]$^+_{(aq)}$ system. [47] Therefore, we decided to examine the mechanism of the olefin epoxidation process by both Bergman's [Cp*MoO$_2$Cl] system (which may also serve as a model for [Cp*MoO$_2$R], R = alkyl, and [Cp*$_2$Mo$_2$O$_5$]), and the [Cp*MoO$_2$]$^+$ ion. Points of interest are:

1) To indentify a low-energy pathway for oxygen transfer from TBHP (or H_2O_2) to the olefin.
2) To understand the difference in catalytic activity between the oxido and peroxido derivatives for Bergman's system, [Cp*MoO$_2$Cl], and [Cp*MoO(O$_2$)Cl].
3) To find possible reasons for the different performances of TBHP and H_2O_2 as oxidants.

It should be noted that the [Cp*MoO$_2$X] system (X = Cl, CH$_3$, Cp*MoO$_3$) is isoelectronic with the [MoO$_2$X$_2$L$_2$] system (see Scheme 5). Thus, the considerations resulting from our calculations on this system may be extrapolated to the more traditional class of [MoO$_2$X$_2$L$_2$] catalysts.

It should also be noted that in a recent contribution, Colbran et al. have shown that a (perarylcyclopentadienyl)molybdenum(VI) dioxido complex, although catalytically active in cyclooctene epoxidation by TBHP, decomposes to a more active non-cyclopentadienyl-containing catalyst as the reaction proceeds.[48] However, an equivalent protonolysis is not necessarily associated also with the more robust[45] Cp*–Mo bond. Furthermore, the isolobal relationship indicated in Scheme 5 makes a mechanistic investigation carried out for the Cp*Mo species also relevant to a putative product of hydrolytic decomposition. A more recent mechanistic study by Kühn et al. on the [CpMoO$_2$(CH$_3$)]-catalyzed epoxidation does not report any catalyst hydrolytic decomposition.[49]

Results and Discussion

Ethylene was used as a model substrate for our computational study (larger olefins, mostly cyclooctene, were used for the experimental studies), and H_2O_2 and MeOOH were the models for the oxidant. However, the full Cp* ligand was maintained in all calculations. The same numbering scheme will be used for the two cycles with different ROOH oxidants. Explicit reference to an individual system will be made by adding R as a superscript, for example, **3^{H}** and **3^{Me}** refer to specific examples of intermediate **3**. Unless otherwise stated, only the solvated energies (E^{CPCM}) will be reported in the figures and discussed (CPCM = conductor-like polarizable continuum model). Related diagrams reporting the relative gas-phase energies are available in the Supporting Information.

Study of the [Cp*MoO$_2$Cl] system (1): As stated in the Introduction, compound [Cp*MoO$_2$Cl] (**1**) was the first reported organomolybdenum olefin epoxidation catalyst, but a theoretical investigation of the catalytic cycle using this compound has, to the best of our knowledge, not been reported. In addition, the corresponding peroxido complex, [Cp*Mo(O$_2$)OCl] (**7**) was described as catalytically inactive,[36,37] but a clear mechanistic interpretation of this phenomenon does not appear to be available. Calculations on this system may also be considered to model the action of other [Cp*MoO$_2$X] catalysts (X = CH$_3$ or Cp*MoO$_3$).[38–41] These molecules are excellent epoxidation catalysts, provided TBHP is used as the oxidant and the solvent is apolar.[42] Chloroform is frequently used, therefore the calculations have been carried out by introducing the solvent effect by the CPCM in CHCl$_3$.

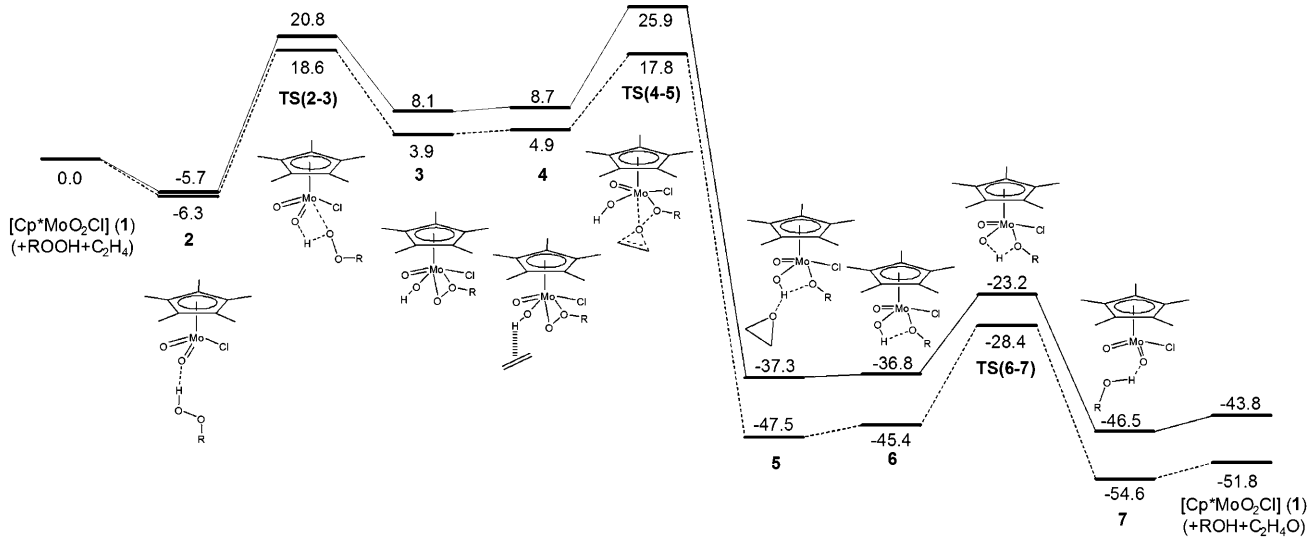

Figure 1. Energy profiles in $CHCl_3$ (in kcal mol^{-1}) for the ROOH activation and C_2H_4 epoxidation by [Cp*MoO_2Cl] (R = H, dashed lines; R = Me, solid lines). The reference energy corresponds to the separate reagents ([Cp*MoO_2Cl] + ROOH + C_2H_4).

On the basis of all previously reported experimental and computational investigations on Mo-catalyzed olefin epoxidation,[2,21–26,28–31,35,43] it is clear that the first step of the catalytic cycle consists of the activation of the oxidant molecule. Therefore, the first step of our investigation was an analysis of the coordination and activation of the ROOH molecule by **1**. The energy profile is shown in Figure 1, and the optimized geometries of the key species are given in Figure 2 for R = Me (corresponding views of the systems with R = H are in the Supporting Information). The starting species **2** features a hydrogen bond between the oxidant as proton donor and an oxido ligand as proton acceptor, slightly stabilizing the system relative to the two separate molecules. The transition state **TS(2–3)** is characterized by nearly equivalent MoO···H and H···OOR distances, more so for **TS(2–3)^{H}**, reflecting an earlier transition state. This structure is quite strained according to the O=Mo–O(H)(OR) angle, 64.7° (65.8° for **TS(2–3)^{H}**), explaining the relatively high activation barrier for this proton-transfer process (26.5 kcal mol^{-1} in $CHCl_3$; 24.9 kcal mol^{-1} for R = H). We found a similar situation in a recent study of the intramolecular proton transfer leading from [Cp*$MoO(OH)_2$]$^+$ to [Cp*$MoO_2(H_2O)$]$^+$.[47] In that case, we found that the barrier could be dramatically reduced by the proton relay action of a water molecule, which is the reaction solvent, because this allows a reduced angular distortion. In $CHCl_3$, the solvent molecules cannot assure a proton relay mechanism, but the same role may be exerted by additional ROOH molecules, and also by the corresponding ROH co-product, once this has started to form, as shown in Scheme 6. Nevertheless, the related proton relay mechanism did not lead to a significant decrease in the energy barrier.

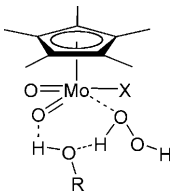

Scheme 6.

This step leads to the formation of the activated complex [Cp*MoOCl(OH)(OOR)] (**3**). Note that **3** displays a significant interaction between the methyl(hydro)peroxido O^{β} atom and the metal center (Mo–O^{β} = 2.830 Å, and Mo-O^{α}-O^{β} = 109.0° for **3^{Me}**; 2.446 Å and 88.7° for **3^{H}**), forming what could be formally described as an alkylated/protonated metal peroxido Mo(η^2-O_2) ligand. It also features a hydrogen bond between the OH ligand as a proton donor and the O^{α} atom of the OOH ligand as a proton acceptor. The nature of this product differs substantially from that obtained in the calculations by Calhorda et al.,[43] in which the two terminally bonded hydroxido and *tert*-butylperoxido ligands in H-O-Mo-O-O-Me establish a hydrogen bond between OH as a proton donor and the O^{β} atom of OOMe as a proton acceptor. It seems that the O^{β} atom prefers to donate its electrons to the electrophilic Mo center than to engage in hydrogen bonding with the OH ligand. Attempts to optimize a structure related to that reported by Calhorda et al. did not lead to a stable minimum for this system. Only two additional minima at slightly higher energy could be located for the R = H system (**3′^{H}** and **3″^{H}**), for which the Mo–OOH moiety is oriented in the opposite direction (namely with a pseudo-equatorial O^{α} atom and a pseudo-axial O^{β} atom) and still features a weak Mo···O^{β} interaction (≈2.8 Å). Views and relative energies of these minima are given in the Supporting Information.

The next step is the oxygen atom transfer from **3** to ethylene. The energy profile is also included in Figure 1, and the transition state geometry is shown in Figure 2. The process starts with the establishment of a weak hydrogen bond between the olefin and the OH ligand (which is essentially thermoneutral: endothermic by 0.6 kcal mol^{-1} for the Me system and by 1.0 kcal mol^{-1} for the H system in $CHCl_3$), forming the adduct **4**. The subsequent step is the transfer of the alkyl(hydro)peroxido O^{α} atom to the olefin through transition state **TS(4–5)**, while the Mo atom strengthens its

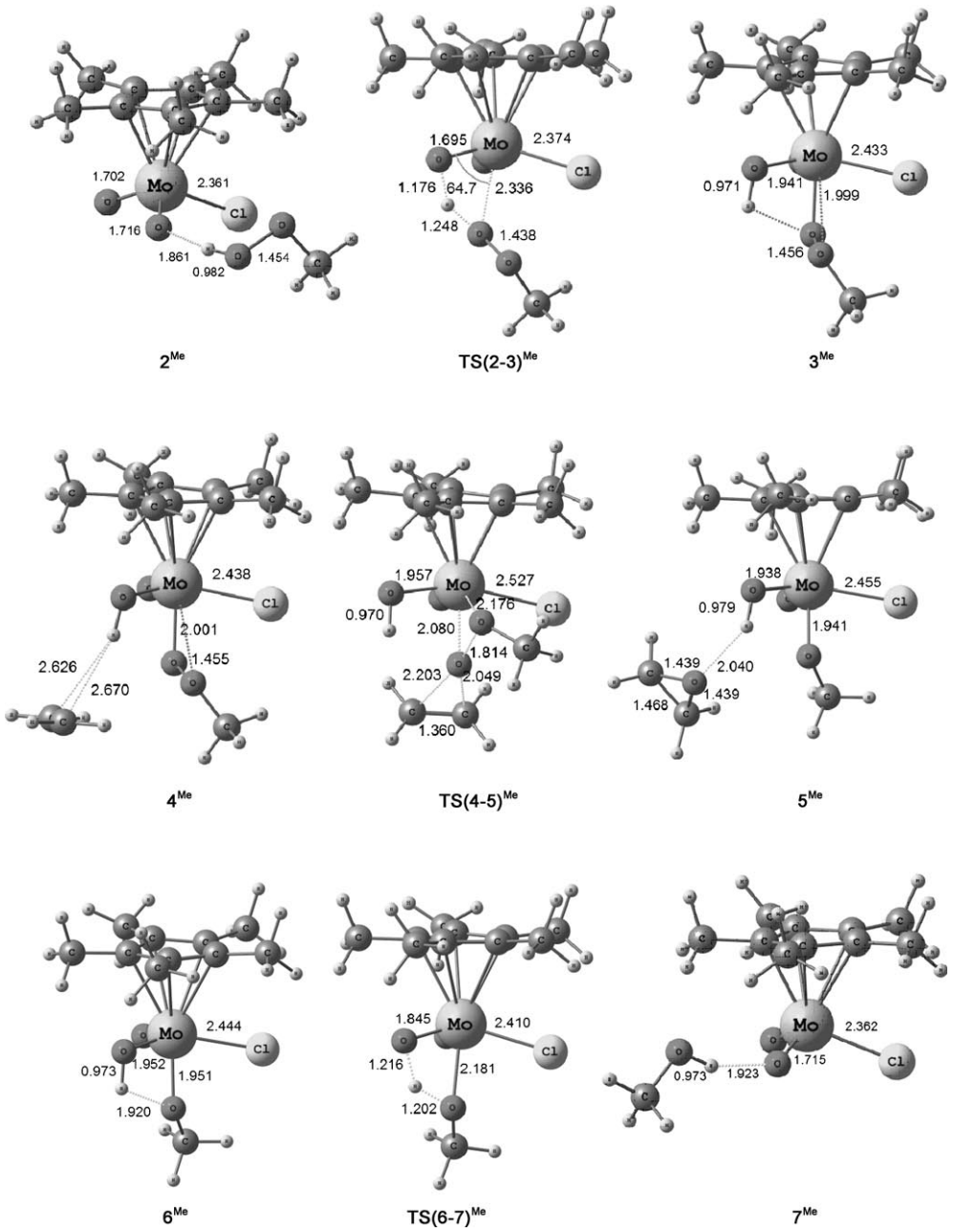

Figure 2. Optimized geometries and main structural data for the systems in Figure 1 (R = Me). Those with R = H are in the Supporting Information.

interaction with the O^{β} atom. The final products, ethylene oxide and [Cp*MoCl(O)$(OH)_2$] (**6**) are formed via the hydrogen-bonded intermediate **5**. The barrier height (17.2 and 12.9 kcal mol^{-1} for the Me and H systems, respectively) appears to be reasonably low for the rate-determining step of an efficient catalytic cycle, and much lower than those estimated earlier for other model systems on the basis of a different mechanism.[35,43] Note that this barrier is significantly affected by the nature of R, most probably because the greater electron-donating power of the Me group renders the O^{α} atom less electrophilic. In order to proceed to a new catalytic cycle, product **6** now needs to eliminate ROH. This process presents an energy barrier of 13.6 and 17.0 kcal mol^{-1} for the Me and H systems in $CHCl_3$, respectively, for a process which is exothermic by 9.7 and 9.2 kcal mol^{-1}, respectively. Thus, it is easier than the initial activation of the catalyst.

To conclude, this pathway for the oxygen transfer step is quite reasonable once ROOH has been activated. The rate-limiting step calculated for the isolated system is the ROOH activation for R = H and the O atom transfer for R = Me, according to the energy profile. However, even for the H system the transition-state energy of **TS(4–5)** is very close to that of **TS(2–3)**, and entropic effects disfavor **TS(4–5)** with respect to **TS(2–3)**, because two species have been added to the system (ROOH and ethylene) in **TS(4–5)** and only one

(ROOH) in **TS(2–3)** (see Supporting Information). From the experimental point of view, all previous kinetic studies yield results consistent with the rate-determining step being oxygen transfer to the olefin,[50–52] including a recent study on a cyclopentadienyl-substituted Mo^{VI} catalyst, [$CpMoO_2(CH_3)$].[49] Thus, our calculated pathway is consistent with experimental observations.

Given the low barriers obtained for the mechanism outlined in Figure 1, we did not consider it worthwhile to explore other pathways, notably those involving the insertion of the ethylene molecule into the Mo–O bond according to the pathway investigated by Calhorda et al.[43] For clarity, the two key steps are compared in Scheme 7. Note that a more recent contribution by Calhorda et al. estimates a much reduced energy for the rate-determining transition state at the MP2 level,[44] which remains, however, higher than the barrier for our pathway. We believe that the O^{β} atom coordination with formation of the strained three-membered MoOO(R) cycle is important for activation of the O^{α} atom. It is possible that the incipient bond formation between the Mo and O^{β} atoms also contributes to the lowering of the activation barrier for the oxygen atom transfer to the olefin. This is presumably achieved by lowering the energy of the O–O σ* orbital, which is susceptible to nucleophilic attack by the external olefin. Indeed, according to a previous study on diperoxo complexes of Group 6 metals, the lower the σ* O–O level, the smaller the activation energy.[21]

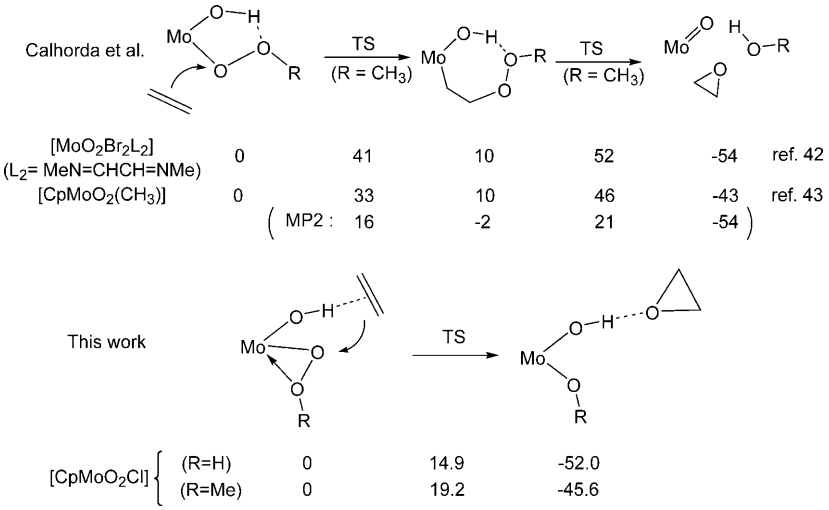

Scheme 7. Comparison of the key (rate-determining) steps of our mechanism and of that reported by Calhorda et al. The relative energies (in kcal mol^{-1}) shown are from the gas phase calculations for comparative purposes.

The mechanism of Figure 1 can therefore be described as a variant of the Sharpless mechanism, in which the oxygen atom is transferred from an alkylperoxido ligand after activation of the oxidant by protonation of an oxido ligand. It is closely related to the mechanism proposed by Thiel (Scheme 3),[32–34] with the peroxido function being replaced by a simpler oxido function as the proton-accepting functionality.

Study of the [Cp*Mo(O_2)OCl] system (8): Next, we proceeded to analyze a possible oxygen transfer process from the peroxido complex [Cp*Mo(O_2)(O)Cl] (**8**), which was found catalytically inactive by the Bergman study.[36] If the peroxido ligand in this complex is already sufficiently activated to transfer an oxygen atom to the exogenous olefin substrate, an elementary process leading to the epoxide product and to the dioxide complex **1** can be envisaged. The latter would then need to be transformed back to **8** by interaction with another oxidant molecule (H_2O_2 or TBHP). The lower energy pathway found for the oxygen-atom-transfer process involves the attack of ethylene at the *exo*-oxygen atom (further away from the Cp* ligand). The transition state **TS(8–1)** is illustrated in Figure 3. The relative energy barrier height for this process is 23.3 kcal mol^{-1} in the gas phase and 23.3 kcal mol^{-1} in $CHCl_3$, namely ≈10 kcal mol^{-1} higher than for the hydroperoxido complex and 5 kcal mol^{-1} higher than for the methylperoxido complex. This result is in good agreement with experimental observation. A possible reason for the higher oxygen transfer barrier for the peroxido (O_2^{2-}) ligand is the higher energy of the O–O σ* orbital relative to that of the ROO^- ligand in complex **3**, as already mentioned above. In previous theoretical work by the groups of Rösch and Frenking it was also concluded that the hydroperoxido mechanism is competitive or superior to the peroxido mechanism.[27,29]

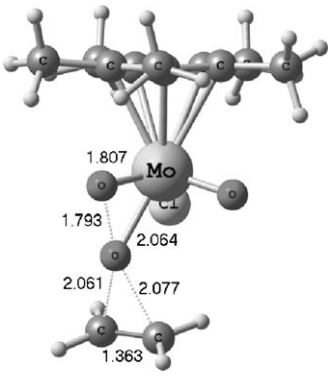

Figure 3. Optimized geometry and main structural data for system **TS(8–1)**.

The above result is not sufficient to dismiss the action of complex **8** as a catalyst, because it can still be envisaged that the peroxido ligand serves as the depository of a proton for

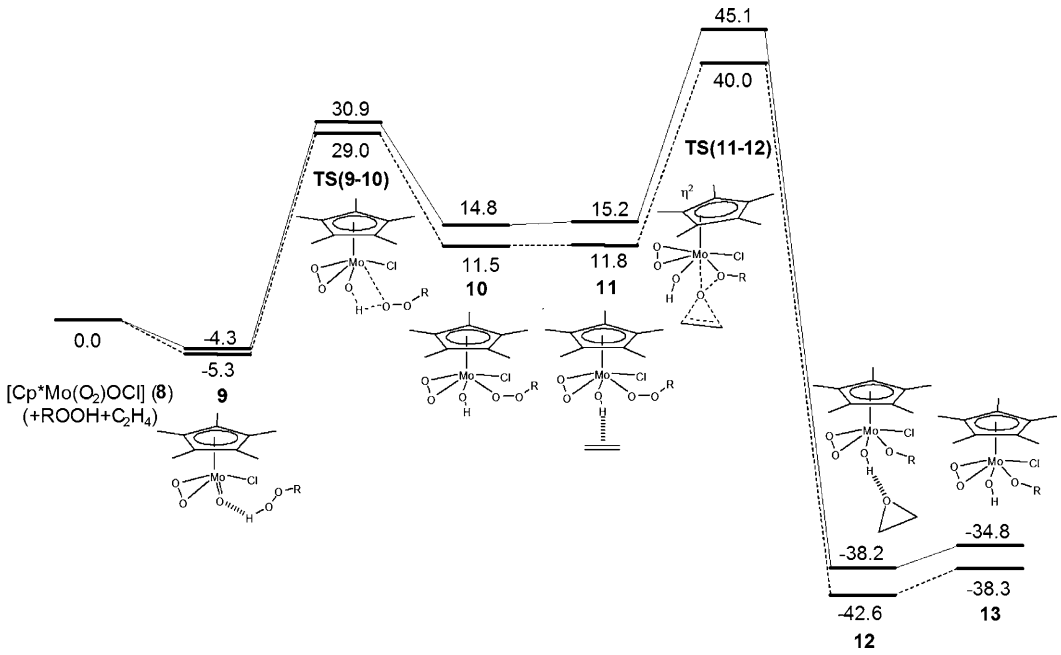

Figure 4. Energy profiles in $CHCl_3$ (in kcal mol^{-1}) for the ROOH activation by [Cp*Mo(O_2)OCl] (R = H, dashed lines; R = Me, solid lines). The reference energy corresponds to the separate reagents ([Cp*Mo(O_2)OCl] + ROOH + C_2H_4).

the activation of another molecule of ROOH in the same way as shown above for the oxido ligand in **1**, as in the pathway suggested by Thiel (Scheme 3).[32–34] The corresponding energy pathway has also been calculated and is reported in Figure 4, with the relevant optimized geometries shown in Figure 5. A quick comparison of Figures 4 and 1 shows that

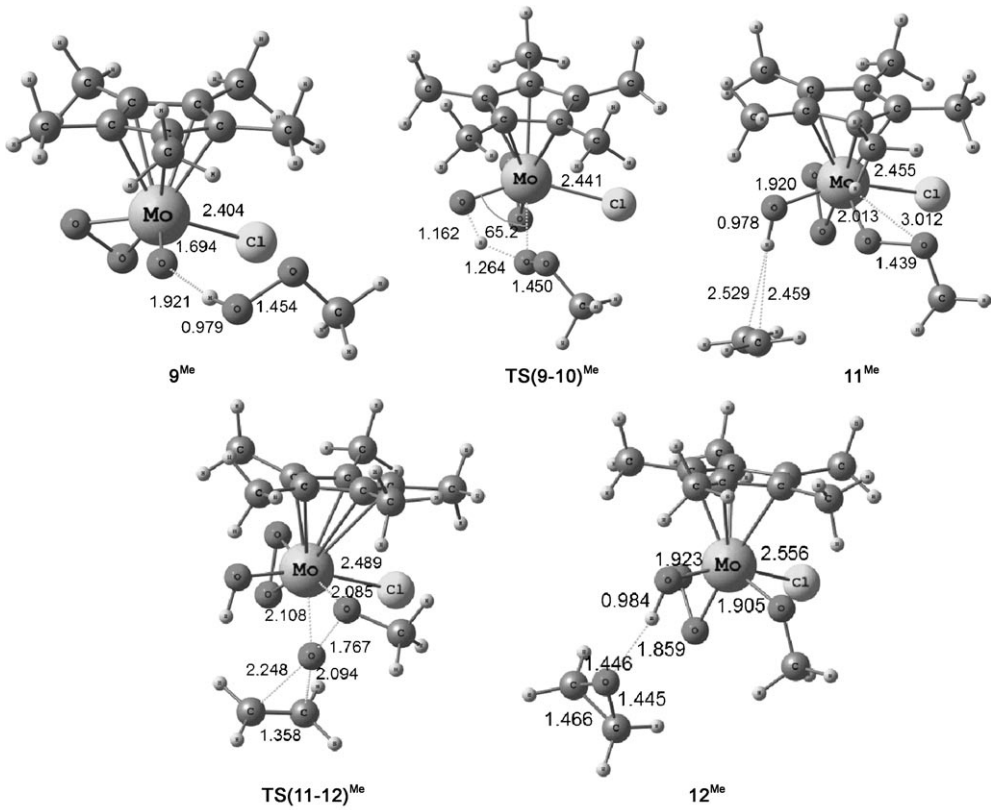

Figure 5. Optimized geometries and main structural data for the systems in Figure 4 (R = Me). Those with R = H are in the Supporting Information.

the Thiel mechanism (involving compound **8** as the active catalyst) is much less favorable than the mechanism involving compound **1**. Both the ROOH activation, **TS(9–10)**, and oxygen transfer, **TS(11–12)**, steps have much greater activation barriers than the corresponding steps for complex **1**, **TS(2–3)** and **TS(4–5)**. The high energy of **TS(9–10)** is somewhat unexpected, since the system is geometrically quite similar to **TS(2–3)** (compare Figures 2 and 5). The much higher barrier for **TS(11–12)** relative to that of **TS(4–5)** may be attributed at least in part to steric compression, as revealed by a greater slip of the Cp* ring in the former transition state. Another important factor may be that the Mo center in the peroxide system is more electron-rich than in the oxido system (O_2^{2-} is a better electron donor than O^{2-}), rendering the Mo···O^{β} interaction weaker. Indeed, in system **10** the Mo–O^{β} distance is much longer (3.008 Å for $\mathbf{10^{Me}}$ and 2.976 Å for $\mathbf{10^{H}}$) and the Mo-O^{α}-O^{β} angle wider (120.9° for $\mathbf{10^{Me}}$ and 119.2° for $\mathbf{10^{H}}$) relative to **3**. A related effect is an energy increase for the O–O σ* orbital, which renders the O^{α} atom less electrophilic. Indeed, the molecular orbitals with the highest σ* O–O contributions are located at 0.144, 1.250, and 1.494 eV for $\mathbf{10^{H}}$, that is, much higher than for $\mathbf{3^{H}}$. Once again, the O transfer step is much less favorable for the Me system than for the H system, because the O atom electrophilicity is reduced by the Me donor power.

The above results also hint as to why certain complexes of type $[Cp^{\#}MoO_2X]$ ($Cp^{\#}$ = substituted cyclopentadienyl ring; X = Cl, alkyl, etc.), as well as isoelectronic $[MoO_2X_2L_2]$ analogues, are efficient for the epoxidation reaction when using TBHP as the oxidant and much less so when using H_2O_2. A direct comparison of the calculated pathways for H_2O_2 and MeOOH in fact shows smaller barriers for the reaction with H_2O_2 in each case. However, the H_2O_2 activation yields a $[Cp^{\#}MoO(OH)(OOH)X]$ intermediate, such as **3**, which may then eliminate water and afford more electron-rich peroxido complexes $[Cp^{\#}Mo(O_2)(O)X]$, such as **8**, the latter being less active catalysts according to the above calculations. This water elimination process has not been investigated computationally for the chloride system, but has been considered for the related cationic system that is discussed in the next section. Note that in some cases, such as the recently investigated $[CpMoO_2(CH_3)]$ system,[49] the resulting peroxo complex is also catalytically active. However, it was shown that the catalytic activity for the TBHP-based epoxidation of complex $[CpMoO(O_2)(CH_3)]$ is lower than that of $[CpMoO_2(CH_3)]$, by an estimated factor of 3–5.[49] An analysis of the reason for the catalytic activity of $[CpMoO(O_2)(CH_3)]$, whereas $[Cp^*MoO(O_2)Cl]$ was found inactive, is beyond the scope of the present investigation, but is probably due to a fine tuning of the activation barriers by the nature of X, and to the different size of the cyclopentadienyl ring.

Study of the $[Cp^*MoO_2]^+$ system: This investigation was prompted by our knowledge of the speciation of compound $[Cp^*_2Mo_2O_5]$ in an aqueous medium,[46,47] and by our recent finding that the compound catalyzes cyclooctene epoxidation by TBHP in the presence of water.[41,42] $[Cp^*_2Mo_2O_5]$ maintains a dinuclear structure in organic solvents, including polar ones such as MeCN and MeOH, but behaves as a weak electrolyte in water, producing $[Cp^*MoO_2(H_2O)]^+$ and $[Cp^*MoO_3]^-$. In addition, water dissociation from $[Cp^*MoO_2(H_2O)]^+$ was found to be rapid and reversible.[47] The electron richness of the anionic complex is likely to preclude H_2O_2 (or TBHP) activation and olefin epoxidation catalysis, but the cationic complex, which is isoelectronic with compound **1**, could lead to epoxidation catalysis. Therefore, we repeated the study described above using this cationic system as a catalyst.

Taking complex $[Cp^*MoO_2(H_2O)]^+$ (**14**) as the starting point, the energy profile limited to the ROOH activation phase is reported in Figure 6. The dissociation of water from

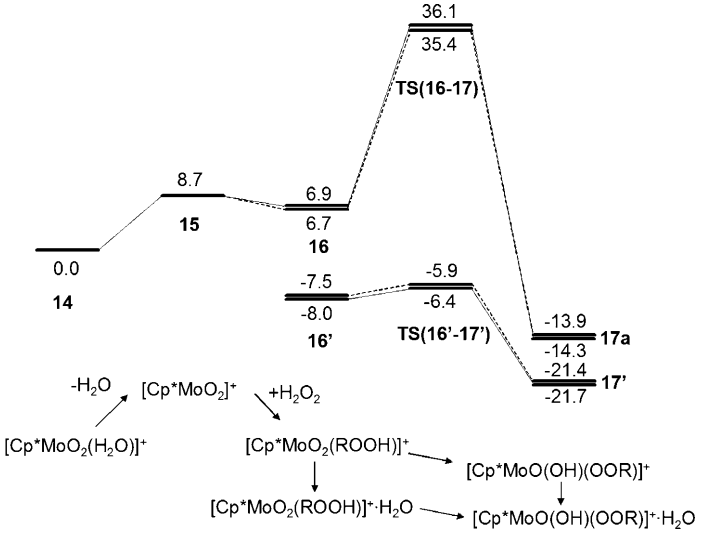

Figure 6. Energy profile in water (in kcal mol^{-1}) for the activation of ROOH (R = Me, solid lines; R = H, dashed lines) by $[Cp^*MoO_2(H_2O)]^+$ (**14**).

$[Cp^*MoO_2(H_2O)]^+$ to yield the coordinatively unsaturated $[Cp^*MoO_2]^+$ species has already been reported in our previous study,[47] and is shown again here for the purpose of comparison. It requires only 8.7 kcal mol^{-1} in water. There is, therefore, a great difference between this cationic complex in water and the isoelectronic $[Cp^*MoO_2Cl]$ complex in $CHCl_3$: Cl^- dissociation from $[Cp^*MoO_2Cl]$ is very energy-demanding (61.7 kcal mol^{-1}) in a non-polar solvent such as $CHCl_3$. This dissociation leaves the coordination position in $[Cp^*MoO_2]^+$ available for H_2O_2 binding and activation.

Coordination of H_2O_2 to this unsaturated species leads to a substitution product **16** that is only slightly destabilized relative to the aqua complex **14**. This different stability reflects the greater donor power of H_2O relative to H_2O_2 and MeOOH. The isomeric $[Cp^*MoO(OH)(OOR)]^+$ species (**17a**) is even lower in energy, being located at −20.6 (for R = H) and −21.2 kcal mol^{-1} (for R = Me) from **16** in water. The optimized geometries for the Me systems are shown in

Figure 7. The Mo–O^{β} distance of 2.391 Å and the Mo-O^{α}-O^{β} angle of 89.2° suggest a significant interaction between Mo and O^{β}, similar to and even stronger than that experienced by complex **3**, as expected from the unsaturated nature of this system.

The intramolecular proton transfer leading from **16** to **17a** requires a rather high activation: 28.7 (R = H) or 29.2 kcal mol^{-1} (R = Me) in water. In this activation, one proton of the ROOH molecule migrates to one oxo ligand, whereas the OOR moiety becomes covalently bonded to the Mo atom. The migrating proton is located approximately midway between the two oxygen atoms in the transition state **TS(16–17)** (also shown in Figure 7). Note that this transition state is related to that obtained for the ROOH activation by **1**, **TS(2–3)** (Figure 2). However, the Mo–O(H)OR bond is already fully formed in the precursor to **TS(16–17)**, whereas it is in the process of being established in **TS(2–3)**. The O-Mo-O angle involving the donating and accepting O atoms in **TS(16–17)** is quite significantly narrowed relative to **16**. This is probably the main reason for such a high activation barrier. Following the same strategy previously used to investigate a similar intramolecular proton transfer process leading from $[Cp^*MoO(OH)_2]^+$ to $[Cp^*MoO_2(H_2O)]^+$,[47] we considered the participation of additional water molecules as proton relay agents.[47,53–56]

Indeed, the addition of just one water molecule is sufficient to dramatically decrease the barrier to only 1.6 kcal mol^{-1} for both R = H and R = Me in solution (see Figure 6). Therefore, the water-assisted pathway should be the preferred one. The additional water lowers the energy of both starting (**16** to **16′**) and final (**17a** to **17′**) systems through the establishment of a hydrogen bond. Thermodynamically, the process is exothermic by 13.9 (R = H) or 13.7 kcal mol^{-1} (R = Me) in water. The related optimized geometries are shown also in Figure 7, including that of the transition state **TS(16′–17′)**, which is relaxed with a O-Mo-OOH angle of 94.8°. An analysis of the various O–H distances shows that the donating O–H bond has already largely broken, whereas the incipient O–H bond has not yet formed to a great extent. Therefore, the transition state may be more correctly described as having a $[Cp^*MoO_2(OOR)]\cdot(H_3O^+)$ character. To conclude this part, the calculations suggest that the ROOH activation process is very facile. The slowest step is the H_2O dissociation from **14**, which requires only 8.7 kcal mol^{-1} in solution, considering a dissociative mechanism.

We now turn to the oxygen transfer step from the activated oxidant to the olefin. Starting from **17a^{H}**, we were able to locate two pathways with practically equivalent activation barriers, for which the transferred oxygen atom is the O^{β} atom in one case (transition state **TS(18–19)^{H}**) and the O^{α} atom in the other case (transition state **TS(21–22)^{H}**). The energy profiles of these two pathways are shown for comparison in Figure 8. The first pathway starts with a hydro-

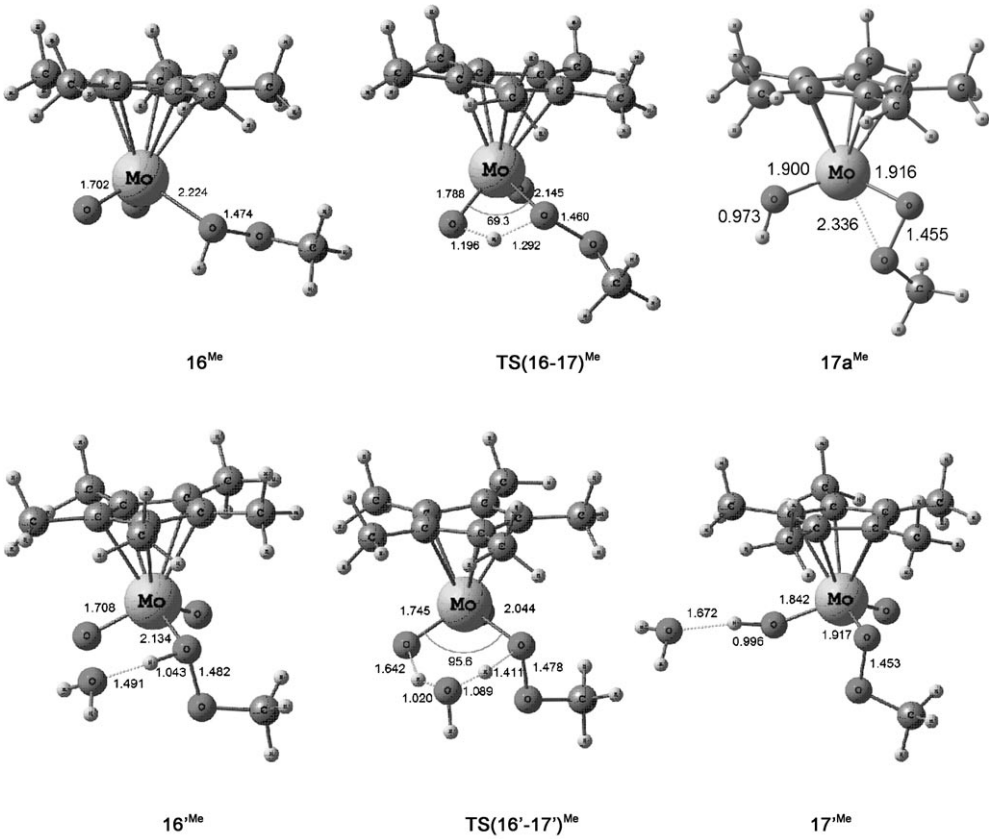

Figure 7. Optimized geometries and main structural data for the systems in Figure 6 (R = Me). Those with R = H are in the Supporting Information.

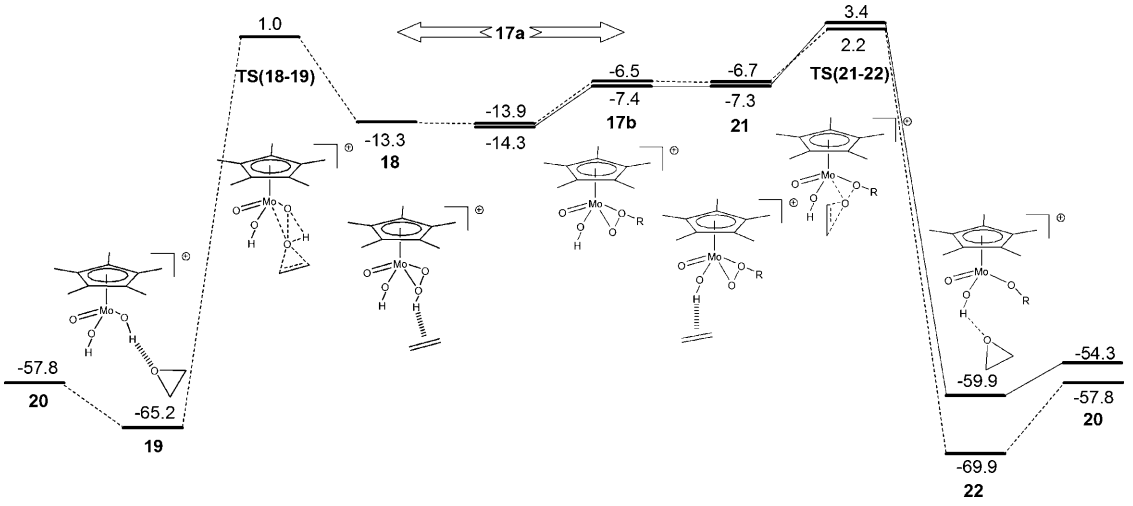

Figure 8. Energy profiles in water (in kcal mol^{-1}) for the oxygen atom transfer from **17a** to ethylene (R = Me, solid lines; R = H, dashed lines).

gen-bonding interaction between the ethylene π-electron density and the hydroperoxido proton, leading to the **18^{H}** structure accompanied by a significant stabilization, and continues with a 1,2-proton shift from the O$^{\beta}$ to the O$^{\alpha}$ atom, leading to the bis(hydroxido) derivative **20** via an intermediate **19** with an hydrogen-bonded epoxide product. This pathway would certainly occur via a prohibitively high-energy transition state when R = Me, therefore calculations along this pathway were not carried out.

Concerning the second pathway (optimized geometries in Figure 9), the first step is an endoergic reorientation of the OOR group (7.4 and 6.9 kcal mol^{-1} for R = H and Me, respectively) from a perpendicular to a parallel arrangement (**17b**), to which the ethylene may attack at the O$^{\alpha}$ atom after an initial approach through an essentially thermoneutral hydrogen-bond with the O–H group. A direct olefin attack at **17a** did not allow us to locate an oxygen transfer pathway. As for compound **1** (Figure 1), the olefin attack is exogenous, without formation of metal–carbon bonds, via the transition state **TS(21–22)**, in which the Mo center strengthens its interaction with the O$^{\beta}$ atom. The transition state **TS(21–22)** for this cationic system is closely related to **TS(4–5)** of the neutral chlorido system **1** (Figure 1). As for **TS(4–5)**, the barrier is slightly higher for the Me system than for the H system, for the same reasons as discussed above. The barrier height (16.1 and 17.7 kcal mol^{-1} for the H and Me systems in water with respect to

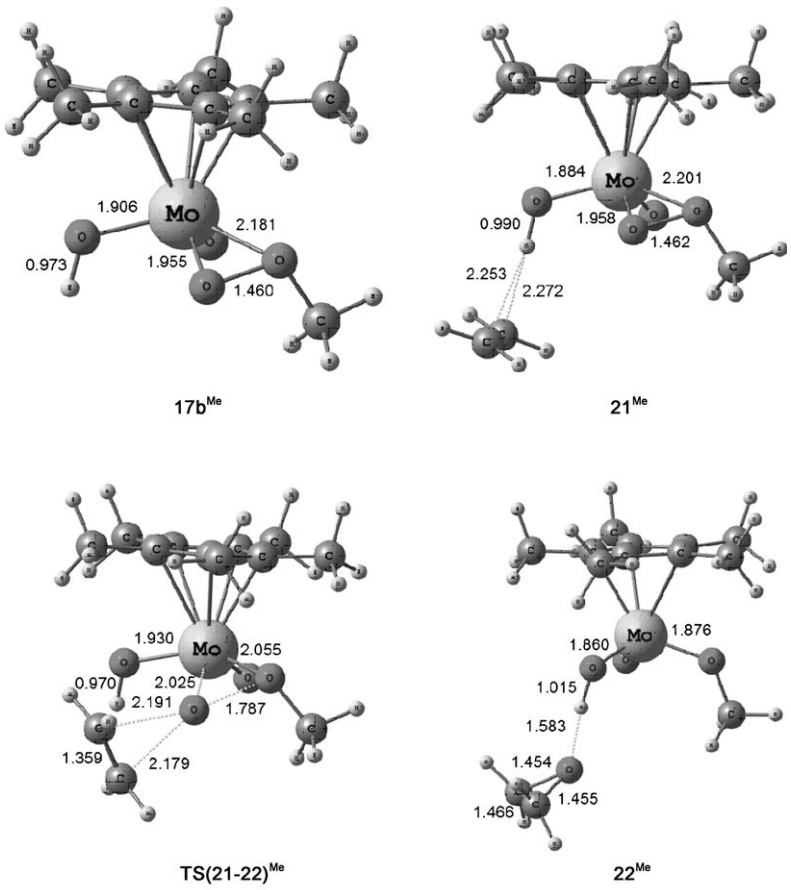

Figure 9. Optimized geometries and main structural data for the systems in Figure 8 (R = Me). Those with R = H are in the Supporting Information.

17a) is also close to the barrier leading to **TS(4–5)** (13.9 and 17.8 kcal mol^{-1} in $CHCl_3$). This pathway leads to the same products, $[Cp^*Mo(O)(OH)_2]^+$ (**20**) and ethylene oxide, because the 1,2-proton shift discussed above, via the hydrogen-bonded intermediate **22**, is only slightly different than **19**. The regeneration of the starting complex **14** by intramolecular proton transfer, assisted by additional water molecules, occurs by a low-energy pathway, as shown in our previous study.[47] Clearly, both pathways are energetically viable, although only that via **TS(21–22)** may take place when using TBHP as the oxidant.

Conclusions

The present study has unveiled a low-energy pathway for olefin epoxidation catalyzed by cyclopentadienyl–Mo^{VI} systems. The initial H_2O_2 activation follows the same general path as described in other recent computational studies,[35,43] with protonation of an oxido ligand and generation of a hydroxide hydroperoxido intermediate, but unlike the previous study the latter is found to adopt an asymmetric η^2 coordination mode, with a weak interaction between the O^β atom and the metal center. This interaction is critical for the activation of the O^α atom toward an exogenous nucleophilic attack by the olefin substrate, leading to significantly lower activation barriers for the oxygen atom transfer to the olefin relative to the previous study. This mechanism closely corresponds to what has been proposed by Thiel et al., except that an oxido ligand is the depository of the oxidant proton rather than a peroxido ligand. An analogous mechanism is found both for $[Cp^*MoO_2Cl]$ (**1**) and $[Cp^*MoO_2(H_2O)]^+$ (**13**) complexes. The study also provides a rationale for the lower activity of peroxido derivatives relative to the oxido analogues, and for the lower activity of H_2O_2 relative to THBP. The former oxidant may undergo isomerization of the reactive hydroperoxido intermediate through proton transfer, leading to less reactive peroxido derivatives. Therefore, the design of an efficient catalytic system for olefin epoxidation by H_2O_2 should only provide a basic site for the transfer of one of the two H_2O_2 protons.

Computational Details

Calculations were carried out using the Gaussian 03 package[57] at the DFT level by means of the B3LYP functional.[58–60] For the Mo atom, the LANL2DZ pseudopotential[61] was used, with the addition of f polarization functions.[62] The 6-31G(d) basis set was used for C atoms, whereas additional diffuse functions [6-31$^+$G(d)] were added for O and Cl atoms due to their anionic character. For the hydrogen atoms, the 6-31G(d,p) basis set was employed. IRC calculations were made in order to obtain the two minima linked by every transition state.[63–65] Solvent effects were included by means of CPCM single point calculations, using chloroform ($\varepsilon = 4.9$ at 25 °C) for the neutral systems and water ($\varepsilon = 78.39$ at 25 °C) for the cationic catalyst.[66,67] For these calculations, an extended basis set was used for C, O, and H: 6-311^{++}G(d,p). Additional spheres were included for all the hydrogen atoms, except for the Cp* hydrogens by means of the SPHEREONH option. Thus, all the presented energies both in the figures and in the text are electronic calculations taking into account solvent effects unless explicitly stated. Both free energy values in the gas phase and in solution can be found in the Supporting Information. Frequency calculations were made in order to check the presence of one imaginary frequency in transition-state geometries.

Acknowledgements

We gratefully acknowledge the European Commission for funding this work through the AQUACHEM Research Training Network (Contract no. MRTN-CT-2003-503864). Support from the Spanish MICINN (Projects CTQ2008-06866-CO2-01 and Consolider Ingenio 2010 CSD2007-00006 and FPU fellowship to A.C.-V.), CNRS (LEA Toulouse-Barcelone project), Generalitat de Catalunya (2009/SGR/68 and LEA project), and CICT (project CALMIP) is gratefully acknowledged. We thank M. J. Calhorda for informing us of her parallel work (reference [44]).

[1] J. W. Schwesinger, T. Bauer in *Stereoselective Synthesis* (Eds.: G. Helmchen, R. W. Hoffmann, J. Mulzer, E. Schaumann), Thieme, New York, **1995**.
[2] B. Lane, K. Burgess, *Chem. Rev.* **2003**, *103*, 2457–2473.
[3] F. E. Kühn, A. M. Santos, W. A. Herrmann, *Dalton Trans.* **2005**, 2483–2491.
[4] C. Freund, M. Abrantes, F. E. Kühn, *J. Organomet. Chem.* **2006**, *691*, 3718–3729.
[5] F. E. Kühn, A. M. Santos, M. Abrantes, *Chem. Rev.* **2006**, *106*, 2455–2475.
[6] C. Freund, W. Herrmann, F. E. Kühn, *Top. Organomet. Chem.* **2007**, *22*, 39–77.
[7] M. J. Calhorda, P. J. Costa, *Dalton Trans.* **2009**, 8155–8161.
[8] M. H. Dickman, M. T. Pope, *Chem. Rev.* **1994**, *94*, 569–584.
[9] N. Mizuno, K. Yamaguchi, K. Kamata, *Coord. Chem. Rev.* **2005**, *249*, 1944–1956.
[10] V. Nardello, J.-M. Aubry, D. E. De Vos, R. Neumann, W. Adam, R. Zhang, J. E. Ten Elshof, P. T. Witte, P. L. Alsters, *J. Mol. Catal. A* **2006**, *251*, 185–193.
[11] J.-M. Bregeault, M. Vennat, L. Salles, J.-Y. Piquemal, Y. Mahha, E. Briot, P. C. Bakala, A. Atlamsani, R. Thouvenot, *J. Mol. Catal. A* **2006**, *250*, 177–189.
[12] T. Katsuki, *Coord. Chem. Rev.* **1995**, *140*, 189–214.
[13] C. T. Dalton, K. M. Ryan, V. M. Wall, C. Bousquet, D. G. Gilheany, *Top. Catal.* **1998**, *5*, 75–91.
[14] E. M. Mcgarrigle, D. G. Gilheany, *Chem. Rev.* **2005**, *105*, 1563–1602.
[15] E. Rose, B. Andrioletti, S. Zrig, M. Quelquejeu-Etheve, *Chem. Soc. Rev.* **2005**, *34*, 573–583.
[16] R. A. Sheldon, J. Kochi, *Metal-Catalyzed Organic Reactions*, Academic Press, New York, **1981**, p. 48.
[17] J. W. Faller, Y. Ma, *J. Organomet. Chem.* **1989**, *368*, 45–56.
[18] G. Wilkinson, R. D. Gillard, J. A. Mccleverty, *Comprehensive Coordination Chemistry*, Pergamon Press, Oxford, **1988**.
[19] H. Mimoun, I. Seree De Roch, L. Sajus, *Tetrahedron* **1970**, *26*, 37–50.
[20] K. B. Sharpless, J. M. Townsend, D. R. Williams, *J. Am. Chem. Soc.* **1972**, *94*, 295–296.
[21] C. Di Valentin, P. Gisdakis, I. V. Yudanov, N. Rösch, *J. Org. Chem.* **2000**, *65*, 2996–3004.
[22] I. V. Yudanov, C. Di Valentin, P. Gisdakis, N. Rösch, *J. Mol. Catal. A* **2000**, *158*, 189–197.
[23] D. V. Deubel, J. Sundermeyer, G. Frenking, *J. Am. Chem. Soc.* **2000**, *122*, 10101–10108.
[24] D. V. Deubel, J. Sundermeyer, G. Frenking, *Inorg. Chem.* **2000**, *39*, 2314–2320.
[25] D. V. Deubel, *J. Phys. Chem. A* **2001**, *105*, 4765–4772.
[26] D. V. Deubel, J. Sundermeyer, G. Frenking, *Eur. J. Inorg. Chem.* **2001**, 1819–1827.

[27] D. V. Deubel, J. Sundermeyer, G. Frenking, *Org. Lett.* **2001**, *3*, 329–332.
[28] D. V. Deubel, G. Frenking, P. Gisdakis, W. A. Herrmann, N. Rösch, J. Sundermeyer, *Acc. Chem. Res.* **2004**, *37*, 645–652.
[29] P. Gisdakis, I. V. Yudanov, N. Rösch, *Inorg. Chem.* **2001**, *40*, 3755–3765.
[30] M. Bühl, R. Schurhammer, P. Imhof, *J. Am. Chem. Soc.* **2004**, *126*, 3310–3320.
[31] L. Salles, J. Y. Piquemal, R. Thouvenot, C. Minot, J. M. Bregeault, *J. Mol. Catal. A* **1997**, *117*, 375–387.
[32] W. R. Thiel, T. Priermeier, *Angew. Chem.* **1995**, *107*, 1870–1871; *Angew. Chem. Int. Ed. Engl.* **1995**, *34*, 1737–1738.
[33] W. R. Thiel, *J. Mol. Catal. A* **1997**, *117*, 449–454.
[34] W. R. Thiel, J. Eppinger, *Chem. Eur. J.* **1997**, *3*, 696–705.
[35] F. E. Kühn, M. Groarke, E. Bencze, E. Herdtweck, A. Prazeres, A. M. Santos, M. J. Calhorda, C. C. Romão, I. S. Gonçalves, A. D. Lopes, M. Pillinger, *Chem. Eur. J.* **2002**, *8*, 2370–2383.
[36] M. B. Trost, R. G. Bergman, *Organometallics* **1991**, *10*, 1172–1178.
[37] D. Chakraborty, M. Bhattacharjee, R. Krätzner, R. Siefken, H. W. Roesky, I. Usón, H.-G. Schmidt, *Organometallics* **1999**, *18*, 106–108.
[38] M. Abrantes, A. Santos, J. Mink, F. Kühn, C. Romão, *Organometallics* **2003**, *22*, 2112–2118.
[39] J. Zhao, A. M. Santos, E. Herdtweck, F. E. Kühn, *J. Mol. Catal. A* **2004**, *222*, 265–271.
[40] J. Zhao, E. Herdtweck, F. E. Kühn, *J. Organomet. Chem.* **2006**, *691*, 2199–2206.
[41] A. M. Martins, C. C. Romão, M. Abrantes, M. C. Azevedo, J. Cui, A. R. Dias, M. T. Duarte, M. A. Lemos, T. Lourenço, R. Poli, *Organometallics* **2005**, *24*, 2582–2589.
[42] Unpublished studies in one of our laboratories by using aqueous H_2O_2 as an oxidant for the $[Cp^*_2Mo_2O_5]$-catalyzed epoxidation of octane have shown that the olefin substrate is consumed rapidly, indicating cayalytic activity, but the amount of produced epoxidation product is very small. The nature of the products obtained under these conditions is currently unknown.
[43] L. F. Veiros, A. Prazeres, P. J. Costa, C. C. Romão, F. E. Kühn, M. J. Calhorda, *Dalton Trans.* **2006**, 1383–1389.
[44] During the drafting of the present manuscript, we have learned from M. J. Calhorda that, by using $[CpMoO_2(CH_3)]$ as catalyst, the activation barrier for the mechanism of Scheme 4 becomes much lower when the calculations were carried out at the MP2 level (single point calculations on DFT optimized geometries had the effect of lowering the highest energy transition state from 50 to only 24 kcal mol^{-1} relative to $[CpMoO_2(CH_3)]+C_2H_4+MeOOH$; P. J. Costa, M. J. Calhorda, F. E. Kühn, *Organometallics*, **2010**, DOI: 10.1021/om9002522.
[45] R. Poli, *Chem. Eur. J.* **2004**, *10*, 332–341.
[46] E. Collange, J. Garcia, R. Poli, *New J. Chem.* **2002**, *26*, 1249–1256.
[47] J.-E. Jee, A. Comas-Vives, C. Dinoi, G. Ujaque, R. Van Eldik, A. Lledós, R. Poli, *Inorg. Chem.* **2007**, *46*, 4103–4113.
[48] M. Pratt, J. B. Harper, S. B. Colbran, *Dalton Trans.* **2007**, 2746–2748.
[49] A. M. Al-Ajlouni, D. Veljanovski, A. Capapé, J. Zhao, E. Herdtweck, M. J. Calhorda, F. E. Kühn, *Organometallics* **2009**, *28*, 639–645.
[50] Y. Nakagawa, N. Mizuno, *Inorg. Chem.* **2007**, *46*, 1727–1736.
[51] A. A. Valente, J. Moreira, A. D. Lopes, M. Pillinger, C. D. Nunes, C. C. Romao, F. E. Kühn, I. S. Goncalves, *New J. Chem.* **2004**, *28*, 308–313.
[52] J. P. Collman, L. Zeng, H. J. H. Wang, A. Lei, J. I. Brauman, *Eur. J. Org. Chem.* **2006**, 2707–2714.
[53] A. Lledós, J. Bertrán, *Tetrahedron Lett.* **1981**, *22*, 775–778.
[54] J. R. Sambrano, J. Andres, L. Gracia, V. S. Safont, A. Beltran, *Chem. Phys. Lett.* **2004**, *384*, 56–62.
[55] R. Prabhakar, M. R. A. Blomberg, P. E. M. Siegbahn, *Theor. Chem. Acc.* **2000**, *104*, 461–470.
[56] H. P. Hratchian, J. L. Sonnenberg, P. J. Hay, R. L. Martin, B. E. Bursten, H. B. Schlegel, *J. Phys. Chem. A* **2005**, *109*, 8579–8586.
[57] Gaussian 03, Revision D.01, M. J. Frisch, G. W. Trucks, H. B. Schlegel, G. E. Scuseria, M. A. Robb, J. R. Cheeseman, J. Montgomery, Jr., J. A., T. Vreven, K. N. Kudin, J. C. Burant, J. M. Millam, S. S. Iyengar, J. Tomasi, V. Barone, B. Mennucci, M. Cossi, G. Scalmani, N. Rega, G. A. Petersson, H. Nakatsuji, M. Hada, M. Ehara, K. Toyota, R. Fukuda, J. Hasegawa, M. Ishida, T. Nakajima, Y. Honda, O. Kitao, H. Nakai, M. Klene, X. Li, J. E. Knox, H. P. Hratchian, J. B. Cross, C. Adamo, J. Jaramillo, R. Gomperts, R. E. Stratmann, O. Yazyev, A. J. Austin, R. Cammi, C. Pomelli, J. W. Ochterski, P. Y. Ayala, K. Morokuma, G. A. Voth, P. Salvador, J. J. Dannenberg, V. G. Zakrzewski, S. Dapprich, A. D. Daniels, M. C. Strain, O. Farkas, D. K. Malick, A. D. Rabuck, K. Raghavachari, J. B. Foresman, J. V. Ortiz, Q. Cui, A. G. Baboul, S. Clifford, J. Cioslowski, B. B. Stefanov, G. Liu, A. Liashenko, P. Piskorz, I. Komaromi, R. L. Martin, D. J. Fox, T. Keith, M. A. Al-Laham, C. Y. Peng, A. Nanayakkara, M. Challacombe, P. M. W. Gill, B. Johnson, W. Chen, M. W. Wong, C. Gonzalez, J. A. Pople, Gaussian, Inc., Wallingford CT, **2004**.
[58] A. D. Becke, *J. Chem. Phys.* **1993**, *98*, 5648–5652.
[59] C. T. Lee, W. T. Yang, R. G. Parr, *Phys. Rev. B* **1988**, *37*, 785–789.
[60] P. Stephens, F. Devlin, C. Chabalowski, M. Frisch, *J. Phys. Chem.* **1994**, *98*, 11623–11627.
[61] P. J. Hay, W. R. Wadt, *J. Chem. Phys.* **1985**, *82*, 270–283.
[62] A. W. Ehlers, M. Boehme, S. Dapprich, A. Gobbi, A. Hoellwarth, V. Jonas, K. F. Koehler, R. Stegmann, A. Veldkamp, G. Frenking, *Chem. Phys. Lett.* **1993**, *208*, 111–114.
[63] K. Fukui, *Acc. Chem. Res.* **1981**, *14*, 363–368.
[64] C. Gonzalez, H. B. Schlegel, *J. Chem. Phys.* **1989**, *90*, 2154–2161.
[65] C. Gonzalez, H. B. Schlegel, *J. Phys. Chem.* **1990**, *94*, 5523–5527.
[66] V. Barone, M. Cossi, *J. Phys. Chem. A* **1998**, *102*, 1995–2001.
[67] M. Cossi, N. Rega, G. Scalmani, V. Barone, *J. Comput. Chem.* **2003**, *24*, 669–681.

Received: October 17, 2009
Published online: January 7, 2010

